Nucleosynthetic vanadium isotope heterogeneity of the early solar system recorded in chondritic meteorites

Sune G. Nielsen[1,2], Maureen Auro[1], Kevin Righter[3], David Davis[4], Julie Prytulak[5,6], Fei Wu[7], Jeremy D. Owens[7]

[1] - NIRVANA laboratories, Woods Hole Oceanographic Institution, Woods Hole, MA, USA

[2] - Department of Geology and Geophysics, Woods Hole Oceanographic Institution, Woods Hole, MA, USA

[3] - NASA JSC, Houston, TX, USA

[4] - Department of Earth Science, Georgia State University, Atlanta, GA, USA

[5] – Department of Earth Science and Engineering, Imperial College London, UK

[6] – Department of Earth Science, Durham University, UK

[7] - Department of Earth, Ocean and Atmospheric Science, National High Magnetic Field Laboratory, Florida State University, Tallahassee, FL 32306, USA

Abstract - Vanadium (V) isotopes have been hypothesized to record irradiation processes in the early solar system through production of the minor ^{50}V isotope. However, because V only possesses two stable isotopes it is difficult to distinguish irradiation from other processes such as stable isotope fractionation and nucleosynthetic heterogeneity that could also cause V isotope variation. Here we perform the first detailed investigation of V isotopes in ordinary and carbonaceous chondrites to investigate the origin of any variation. We also perform a three-laboratory inter-calibration for chondrites, which confirms that the different chemical separation protocols do not induce V isotope analytical artifacts as long as samples are measured using medium resolution multiple collector inductively coupled plasma mass spectrometry (MC-ICPMS). Vanadium isotope compositions ($^{51}V/^{50}V$) of carbonaceous chondrites correlate with previously reported nucleosynthetically derived excesses in ^{54}Cr. Both ^{51}V and ^{54}Cr are the most neutron-rich of their respective elements, which may suggest that pre-solar grains rich in r-process isotopes is the primary cause of the V-Cr isotope correlation. Vanadium isotope ratios of ordinary chondrite groups and Earth form a weaker correlation with ^{54}Cr that has a different slope than observed for carbonaceous chondrites. The offset between carbonaceous and non-carbonaceous meteorites in V-Cr isotope space is similar to differences also reported for chromium, titanium, oxygen, molybdenum and ruthenium isotopes, which has been inferred to reflect the presence in the early solar system of two physically separated reservoirs. The V isotope composition of Earth is heavier than any meteorite measured to date. Therefore, V isotopes support models of Earth accretion in which a significant portion of Earth was formed from material that is not present in our meteorite collections.

1. Introduction

The early solar system was chemically heterogeneous on both temporal and spatial scales, which is exemplified when comparing the icy outer and rocky inner solar system that preserve major, and minor elemental and isotopic differences (Morbidelli et al., 2000; Morbidelli et al., 2012; Robert et al., 2000). However, the compositional heterogeneity not only spans the vast distances between planets, it can also be observed for different chondritic meteorites (e.g.Burkhardt et al., 2011; Carlson et al., 2007; Clayton, 1993; Qin et al., 2010; Trinquier et al., 2007; Trinquier et al., 2009) as well as in different components of individual chondrites (Clayton, 1993; Gerber et al., 2017; Trinquier et al., 2009; Zinner, 1998). In particular, there has been substantial focus on isotopic differences between meteorites and the origin of such variations (Burkhardt et al., 2011; Carlson et al., 2007; Qin et al., 2010; Trinquier et al., 2009). Much of the isotopic variation can be explained through heterogeneous distribution/thermal mobilization within the solar system of various presolar particles that preserve extremely large isotope anomalies (e.g. Zinner, 1998). These particles constitute a very small fraction of bulk meteorites and hence produce overall relatively small bulk meteorite/planetary isotope heterogeneity.

Alternative processes have been suggested to produce both stable and radiogenic isotope heterogeneity within the early solar system. In particular, high fluxes of charged particles that likely emanated from the young sun (Feigelson, 2010; Shu et al., 1997; Shu et al., 2001) could have caused irradiation of solar system material, producing an array of stable and radioactive isotopes (Gounelle et al., 2006; Lee et al., 1998), although the probability of such processes have been questioned (Desch et al., 2010; Wood, 2004). If irradiated material became heterogeneously distributed in early formed solids, such as calcium aluminum rich inclusions (CAIs) or

chondrules, then their isotopic anomalies could theoretically have been heterogeneously distributed within meteorites or potentially even on planetary scales. To date, however, the best evidence for such processes has primarily been observed for the radioactive isotope ^{10}Be (Chaussidon et al., 2006; McKeegan et al., 2000), whereas other isotopes have been difficult to confirm as originating from early solar system irradiation (Desch et al., 2010; Shen et al., 1994).

Vanadium (V) isotope systematics are susceptible to the production of significant isotope anomalies by irradiation processes because high-energy irradiation can produce the light isotope, ^{50}V, mainly from the target nuclei ^{48}Ti, ^{49}Ti, ^{50}Ti and ^{52}Cr (Burnett et al., 1965; Gounelle et al., 2006; Hopkins et al., 2018; Lee et al., 1998; Sossi et al., 2017). The first high-precision V isotope data for meteorites found that, on average, meteorites were isotopically lighter by ~1‰ compared to estimates for the Bulk Silicate Earth (BSE) (Nielsen et al., 2014). However, since V has only two isotopes, it was not possible to distinguish between mass dependent (e.g. isotope fractionation processes) and independent (e.g. irradiation or nucleosynthetic anomalies) isotope effects. Therefore, it was difficult to determine the exact cause for the V isotope difference between Earth and meteorites. Here, we perform a more detailed investigation of V isotope compositions in chondritic meteorites, including the first data for enstatite chondrites. We employ improved chemical separation and V isotope measurement procedures compared to the previous meteorite work, alongside an inter-lab calibration of two meteorite samples amongst three labs using different analytical protocols. Our re-examination of the V isotope composition of chondritic materials aims to determine if chondrites preserve V isotope variations and, if so, what the likely origin of V isotope heterogeneity in chondrites is.

2. Methods

2.1. Sample preparation

All samples were dissolved as ~100mg chips. Either directly as received from Harvard Museum of Natural History (HMNH) or NASA-JSC by breaking off small chips from larger pieces of meteorite. All samples were free of fusion crust and saw marks. The chips were rinsed in MQ H_2O to remove surficial dust and first dissolved in 1:1 concentrated HNO_3-HF in teflon beakers on a hotplate at ~130°C overnight. The samples were ultrasonicated repeatedly to ensure all silicates became exposed to the HF solution. After evaporation, 5ml of concentrated HNO_3 was added and samples were placed in quartz vessels for further dissolution in an Anton Parr high pressure asher (HPA) at 260°C and ~100 bars pressure for 2.5 hours. This treatment effectively attacks both fluorides remaining after the HF dissolution and refractory minerals that are not easily dissolved. After the HPA treatment samples were transferred back into teflon vials, evaporated, and re-suspended in concentrated HNO_3 and fluxed until no residues were visible in the samples. Treatment with aqua regia and further sonication was applied as necessary to fully dissolve the samples. The only exception was the enstatite chondrite, St Marks, where a residue of graphite was still present after two digestions in the HPA. Finally, each sample was dissolved in 1.3ml 0.8M HNO_3 in preparation for liquid ion exchange chromatography.

2.2. Interlaboratory comparison of contrasting ion exchange chromatography procedures

To investigate whether any analytical artifacts to meteorite analysis may be introduced by different chemical separation procedures, we undertook an inter-laboratory comparison of two meteorites that were analysed in three labs: Woods Hole Oceanographic Institute (WHOI),

Florida State University (FSU) and Imperial College London (ICL). All samples (both for the inter-lab comparison and the wider WHOI dataset) were digested in the NIRVANA laboratory at WHOI as described in 2.1. Splits of digested comparison samples were sent to ICL and FSU. Samples processed at ICL purposefully employed the exact chemical separation procedure described in Nielsen et al. (2011) to allow direct comparison with the meteorite data in Nielsen et al. (2014).

The yields in all three labs were monitored by comparing the amount of V recovered from the column procedure with that expected based on the concentrations measured using ICP-MS (Table S2 and S3). All samples had yields between 85 and 100%. Total procedural blanks were also monitored for each set of samples processed and were always <2ng, which is insignificant compared with the amount of V processed (>1000ng) and thus no blank correction is required.

The chemical separation procedures used at WHOI and FSU labs rely on the same principles as those outlined by Nielsen et al (2011) and Wu et al (2016), but differ in some details. In the following we outline the key differences between chemical separations and mass spectrometric protocols.

2.2.1. WHOI chemical separation of V

The total procedure involved four individual ion exchange columns. The first column used AG 50W-X8 cation exchange resin and was a modified version of the cation exchange column presented in Wu et al (2016). In the modified version, 3ml of AG 50W-X8 cation resin is loaded into quartz columns with a stem inner diameter of 6mm and ~150mm height. In principle, the AG 50W-X12 resin utilized by Wu et al (2016) has a larger sample capacity and is, therefore, a more flexible procedure as it places less strict limits on the amount of sample that can be processed. However, AG 50W-X12 is more expensive than AG 50W-X8 and the two resins

otherwise operate very similarly. After resin had been loaded it was cleaned with 10ml of 50% HNO_3 and then re-equilibrated with 3x4ml of 0.8M HNO_3. Onto each column 1.3ml of sample in 0.8M HNO_3 was loaded. Subsequently, 2x3ml of 0.1MHF+0.8M HNO_3 was added to remove Ti and Al. This step was followed by elution of V in 29ml of 0.8M HNO_3. As also outlined in Wu et al (2016) we find that all major elements except for Na and K are retained on the column while V is eluted quantitatively. However, our column also effectively separates Mg from V, perhaps because 0.8M HNO_3 is used as opposed to 1M HNO_3 (Wu et al., 2016). Varying amounts of sample mass (e.g. total mg rock) or V mass (e.g. total μg of V) loaded onto the column shifts the V elution peak (Wu et al., 2016) and therefore the sample mass loaded was restricted to between 10-20mg and the total mass of V loaded onto the column never exceeded 6μg. Following the cation exchange column, samples were evaporated to dryness, refluxed in aqua regia overnight at 135°C, evaporated, refluxed in 1:1 nitric acid:hydrogen peroxide, evaporated at 135°C and finally converted to chloride form by fluxing in HCl. Samples were then redissolved in ~10ml 0.01M HCl in preparation for the anion exchange column that uses 1ml AG1-X8 resin. Here we followed the same procedure as outlined in Nielsen et al (2011) where addition of H_2O_2 to the samples immediately before loading onto the column results in V strongly binding to the resin. After the 1ml anion exchange column we repeated the same anion column in miniaturized form twice using 0.15ml of AG1-X8 resin. The only modification for the miniaturized columns was that we eluted matrix elements (trace Cr and Ti) in 0.1M HCl+2% H_2O_2, which we found removed the remaining trace Ti more effectively than 0.01M HCl+2% H_2O_2 without incurring any loss of V. However, even with the more efficient Ti removal, we found that two miniaturized 0.15ml AG1-X8 resin columns were required to remove Cr

154 effectively, which is likely due to the very high Cr/V ratios (~25-80) found in most chondritic
155 meteorites compared with Cr/V <1 found in most terrestrial rocks (except peridotites).

156 *2.2.2. FSU chemical separation of V*

157 The purification of V was conducted with a four-step ion-exchange procedure by coupling
158 cation- and anion-exchange columns after Wu et al., (2016), with only minor modification as
159 shown below. For the cation resin AG50W-X12 (200-400 mesh), we load samples in 1ml of
160 0.8M HNO_3 and then elute matrix elements with 2x2ml of 0.8M HNO_3+0.1M HF and then 1ml
161 of 0.8M HNO_3. Vanadium was then collected with 19 ml of 1.2M HNO_3. The cation-exchange
162 column is run twice to fully remove matrix elements, especially Ti and Fe. For each sample the
163 aliquots before and after the "V-cut" were collected to monitor for any V-loss during the
164 chromatography process. Following the cation exchange column, samples were evaporated and
165 refluxed in aqua regia overnight at 135°C and then evaporated. Samples were then re-dissolved
166 in 1ml 0.01M HCl, which is ready for the anion exchange column that uses 1.4ml AG1-X8 resin
167 as described by Wu et al., (2016). A mini-column with 0.1ml AG1-X8 resin column was then
168 applied to further remove Cr exactly as described in section 2.2.1. Yields and blanks for the FSU
169 separation procedure were similar to those generated at WHOI.
170
171 *2.3. Vanadium isotope composition measurements*

172 The major analytical difference between the original method of Nielsen et al. (2011)
173 compared with almost all subsequent techniques is that the original method employed low mass
174 resolution ($\Delta M/M \sim 400$) whilst subsequent studies used medium mass resolution ($\Delta M/M \sim$
175 4000) where all major molecular interferences can be resolved (Hopkins et al., 2018; Nielsen et
176 al., 2016; Schuth et al., 2017; Sossi et al., 2017; Sossi et al., 2018; Wu et al., 2016). Medium

resolution was not practical during analytical development at Oxford because of the much lower transmission for the Nu Plasma HR MC-ICPMS (~0.5 nA for a solution with 1 μg/ml V(Nielsen et al., 2011) compared with the ThermoFinnegan Neptune MC-ICP-MS whose low resolution V transmission is more than 10 times higher.

2.3.1 Mass spectrometry at WHOI and FSU

All samples were analyzed using MC-ICPMS. The labs at FSU and WHOI house Thermo Scientific Neptune instruments. Sample analysis protocols were similar at WHOI and FSU and follow standard-sample bracketing procedures as described previously (Nielsen et al., 2011) and used desolvating nebulizer systems (Aridus II desolvator) that produced ion beam intensities in medium resolution mode of ~1.5-3 nA ^{51}V for a solution with 1 μg/ml V (Nielsen et al., 2016). The isotopes of mass 49, 50, 52 and 53 are collected with conventional 10^{11} Ω resistors, whereas mass 51 is collected with a 10^{10} Ω resistor to accommodate the ions beams >1nA from ^{51}V.

Vanadium isotope compositions are reported relative to the Alfa Aesar (AA) V specpure solution (Lot #91-092043G) introduced by Nielsen et al. (2011) in conventional permil notation as:

$$\delta^{51}V_{AA} \text{ (in ‰)} = 1000 \times [(^{51}V/^{50}V_{sample} - {}^{51}V/^{50}V_{AA})/^{51}V/^{50}V_{AA}]$$

Interspersed between each sample are analyses of a BDH chemicals vanadium solution, which has an isotope composition of $\delta^{51}V_{AA}$ = -1.20 based on analyses in 7 different labs worldwide (Nielsen et al., 2016; Nielsen et al., 2011; Prytulak et al., 2017; Schuth et al., 2017; Sossi et al., 2017; Sossi et al., 2018; Wu et al., 2016).

In order to correct for isobaric interferences of ^{50}Ti and ^{50}Cr on ^{50}V we monitored ^{49}Ti, ^{52}Cr and ^{53}Cr. To correct accurately for these interferences it is necessary to use a mass bias

correction on the $^{49}Ti/^{50}Ti$ and $^{53}Cr/^{50}Cr$ isotope ratios (Nielsen et al., 2011; Wu et al., 2016) because the ion beams of Ti and Cr are so small that a precise mass bias coefficient cannot be determined during the V isotope measurements. As previously described (Wu et al., 2016), we monitored the mass bias of Cr and Ti by measuring pure 50 ng/ml Alfa Aesar specpure solutions every time the mass spectrometer was re-tuned. The obtained mass bias coefficients were then used to calculate the true ^{50}Ti and ^{50}Cr ion beam that were subtracted from the total signal on mass 50. Due to the efficient separation of V from Cr and Ti these corrections were always less than 15‰ with the majority <5‰. These levels of interferences are relatively simple to correct for precisely and accurately and various doping tests as well as agreement between different labs for USGS reference materials (Prytulak et al., 2011; Wu et al., 2016) have shown that these corrections do not compromise data quality.

2.3.2 Mass spectrometry at ICL

Similar to WHOI and FSU, V isotope measurements at ICL were also made by MC-ICPMS, but instead employing a Nu II Instrument. Samples were introduced via a glass expansion nebulizer with an uptake rate of ~ 120 µl/min followed by desolvation via a Nu instruments DSN 100. Measurements were made by sample-standard bracketing as described in Nielsen et al. (2011) with the same AA solution as above. Analyses of the secondary solution standard BDH were interspersed with the unknown meteorite samples. Samples were run in medium resolution as 600 ng/ml solutions, yielding typical ion beam intensities for ^{51}V of ~0.4 nA for a solution with 1 µg/ml.

The Nu II instrument at ICL is equipped with three $10^{12}\Omega$ resistors, upon which the signals for masses 53, 50 and 49 are collected whilst all other masses of interest (52, 51) are collected on

223 standard $10^{11}\Omega$ resistors. Instead of measuring pure Cr and Ti solutions at the beginning of an
224 analytical session and applying it to all subsequent measurements (Wu et al., 2016; Nielsen et al.,
225 2016), we are able to more precisely measure the minor ^{49}Ti and ^{53}Cr beams using $10^{12}\Omega$
226 resistors to derive and account for the isobaric contribution of ^{50}Cr and ^{50}Ti on the minor ^{50}V
227 isotope. For the case of the meteorite samples, the extended chemical procedure of Nielsen et al.
228 (2011) is very efficient at removal of Cr and Ti such that the magnitude of the Cr and Ti
229 correction from raw $^{51}V/^{50}V$ ratio to Cr and Ti corrected $^{51}V/^{50}V$ ratio was always on the order of
230 0.6‰, and always less than 1.0‰.
231
232
233 **3. Comparison with previous studies and interlaboratory calibration**
234 The V isotope compositions of two carbonaceous chondrites investigated here (EET 92002
235 and ALH 83100) were reported previously (Nielsen et al., 2014). The values obtained for these
236 two chondrites, as well as all other chondrites studied here (Table 1), exhibit V isotope
237 compositions that are significantly heavier by up to 0.9‰ compared with previous chondrite data
238 (Nielsen et al., 2014). Indeed, all bulk compositions of chondrites determined here are
239 significantly heavier than previously reported (Nielsen et al., 2014). In order to assess the
240 precision and accuracy of the new measurements for chondrites, we undertook an inter-
241 laboratory calibration of two chondrites (NWA753 and DOM 08006) to offer some clues to the
242 cause of the discrepancy.
243 The results of these analyses (Table 2), show very good agreement between the labs, despite
244 the different chemical separation protocols (Section 2). Hence there is clearly a systematic
245 difference between the two meteorite data sets that appears unrelated to the samples chosen for

study, any potential meteorite heterogeneity, or the chemical separation protocol. We suggest that the most likely explanation for the disagreement between the data from Nielsen et al. (2014) and the current work is related to the different mass spectrometric protocols employed in Nielsen et al. (2014). These protocols utilized low resolution mass spectrometry, which does not allow separation of polyatomic isobaric interferences. Therefore, the ion exchange chemical separation procedures must effectively remove elements that can generate polyatomic interferences. As shown previously, different sulfur-oxygen (S-O) molecules produce interferences that uniformly make V isotope compositions appear lighter than they are (Nielsen et al., 2016). This effect was inferred to be minor on the Nu Plasma (Nielsen et al., 2011), but is much more pronounced for the Neptune due to its higher transmission efficiency of low-mass elements (Nielsen et al., 2016). In medium resolution mode, however, S-O interferences are separated efficiently from all monitored isotopes of V, Ti and Cr such that even if some sulfur remains in the sample matrix, then S-O interferences have a negligible effect on the measured V isotope ratios. This conclusion is underscored by the fact that there is no difference in V isotope compositions for the interlab calibration samples despite WHOI and FSU utilizing cation exchange resin, which effectively removes sulfate from the sample V, whereas ICL purposefully processed the inter-laboratory meteorite samples with the original chemical separation procedure of Nielsen et al. (2011) for comparison, making it likely that some S remained in the separated V fraction. The agreement between WHOI, FSU and ICL for the meteoritic samples despite their different separation protocols and instrumentation strongly supports that the root of the discrepancy in isotopic composition is directly related to the fact that low resolution measurements are affected by remaining S in the V fraction, an issue exacerbated in S-rich samples such as chondritic meteorites.

It is notable that every attempt was made to rigorously evaluate the previous meteorite data for analytical artifacts both by analyzing multiple replicates of all samples and by conducting a spike addition test for the CV carbonaceous chondrite Allende whereby splits of dissolved meteorite and spike in variable proportions were mixed prior to V separation (Nielsen et al., 2014). The data obtained for these mixing experiments produced a mixing line between the artificially ^{50}V-enriched spike (VISSOX, see Prytulak et al. 2011) and Allende V, which suggested that analytical artifacts were likely minor. The uncertainties on individual Allende-spike mixtures in this first high precision V isotope dataset were relatively large (2SD 0.09-0.42‰) such that a robust York regression (York et al., 2004) of the Allende-spike mixture isotope data that also utilizes 10% (2sd) errors on the concentration of Allende returns a best estimate for unspiked Allende of $\delta^{51}V_{AA}$ = -1.79 ± 0.69‰ (Table S1), which is within error of the value obtained for CV3 chondrites measured here of $\delta^{51}V_{AA}$ = -1.13 ± 0.04‰ (Table 1). However, in all likelihood the Allende-spike mixtures were also affected by ~0.3-0.6‰ analytical artifacts due to insufficient separation of sulfur from sample vanadium, which caused the obtained mixing line to artificially regress close to the value obtained for unspiked Allende measurements (e.g. $\delta^{51}V_{AA}$ = -1.66 ± 0.13‰). This highlights that it is possible to encounter systematic errors on stable isotope measurements that, even when conducting spike addition tests, appear to produce accurate data. With hindsight, in the case of the analytical artifacts on Allende-spike mixtures, it may have been relatively simple to detect these if a larger proportion of the total V (e.g. >80%) processed was spike, because offsets to lighter values might have precluded regression of the data through the isotope composition of the pure spike.

Addition of the cation exchange chromatographic column (Wu et al., 2016) has improved not only separation of most major elements but also aided efficient removal of S, which must

292 further diminish any S-based isobaric interferences or mass bias matrix effects. Importantly,
293 however, non-spectral matrix effects from S-based compounds do not appear to have any notable
294 effect as long as samples are analyzed in medium resolution, as illustrated by the excellent
295 agreement with results from ICL without a cation exchange chromatographic column.

296 Finally, it appears that only previously published meteorite data were compromised by
297 significant S-O interferences. Measurement of S-poor terrestrial silicate reference materials show
298 good agreement between the original low resolution method (Prytulak et al., 2011), studies using
299 medium resolution (Schuth et al., 2017; Sossi et al., 2018; Wu et al., 2018b; Wu et al., 2016),
300 and new measurements of reference materials processed alongside the meteorite comparison
301 samples (Table 3). The largest variance in $\delta^{51}V$ of about 0.33‰ is found in BCR-2, which could
302 have been contaminated during processing in steel jaw crushers and other metal-rich equipment
303 (Woodhead and Hergt, 2000). Since measurements of this reference material were not made
304 from the same jar, it is possible that the observed variance is explained by powder heterogeneity.
305 Certainly, the agreement of multiple jars of BIR1a and BHVO-2 is notably superior to BCR-2.
306 Overall, given the excellent agreement with terrestrial silicate reference materials made in
307 multiple labs by multiple techniques, it is very unlikely that terrestrial silicates measured with the
308 original low resolution MC-ICPMS technique have been significantly impacted, which is also
309 underscored by the agreement between the original and recent measurements of mid ocean ridge
310 basalts (Prytulak et al., 2011; Prytulak et al., 2013; Prytulak et al., 2017; Wu et al., 2018b).
311

312 **4. Discussion**

313 We present results for 10 carbonaceous chondrites and 11 ordinary chondrites. Overall the
314 data displays variation of ~0.3‰ (Table 1) with about the same variation observed for ordinary

315 and carbonaceous chondrites. By comparison, the V isotope variation in chondrites is much
316 smaller than what has been reported for terrestrial samples, which span more than 2‰ (Prytulak
317 et al., 2013; Prytulak et al., 2017; Wu et al., 2018a; Wu et al., 2018b; Wu et al., 2016). However,
318 most of the terrestrial variation likely originates from isotope fractionation that occurs in
319 environments where the multiple different valence states of V (V^{2+}, V^{3+}, V^{4+} and V^{5+}) can
320 partition isotopes between different reservoirs (Wu et al., 2015). Since bulk chondrites show
321 little evidence of processes that are governed by variable redox, it is not surprising that terrestrial
322 samples register much more V isotope variation that bulk chondrites.
323 Given the external measurement uncertainties, most of the data are within error of each
324 other, which can be computed as an overall V isotope composition for chondrites of $\delta^{51}V_{AA}$ = -
325 1.20 ± 0.22 (2sd). However, if the majority of the measurement uncertainty arises from counting
326 statistical errors (Nielsen et al., 2016), then we can calculate 2se errors for groups of meteorites
327 that are likely to be characterized by identical V isotope compositions (e.g. classes of
328 carbonaceous and ordinary chondrites that likely represent the same parent body). This means of
329 assigning error is further supported by the fact that different meteorites from the same group are
330 all within error of each other. With these uncertainties calculated for each group of carbonaceous
331 chondrites investigated there are significant differences in V isotope composition between
332 several of the groups (Table 1). These V isotopic variations could be due to stable isotope
333 fraction, variable proportions of irradiated components (most likely refractory inclusions) or
334 heterogeneous distribution of nucleosynthetically anomalous material. In the following we
335 investigate each of these three possibilities and discuss them in the context of literature data.
336

337 *4.1. Stable isotope fractionation processes*

338 Bulk chondritic meteorites can preserve signatures of stable isotope fractionation processes
339 most commonly through either metamorphic/metasomatic redistribution on a parent body
340 (Wombacher et al., 2008) or due to nebular condensation/evaporation processes during formation
341 of the parent body (Moynier et al., 2011). The elements most susceptible to these processes are
342 either relatively volatile or mobile in fluids. Since V is both relatively refractory (T_c(50%) ~1430
343 K) and immobile during aqueous alteration (Kelley et al., 2003; Lodders, 2003; Prytulak et al.,
344 2013), it is not expected that V isotopes were fractionated by either metamorphic/metasomatic or
345 condensation/evaporation processes that operated during the accretion of chondritic parent
346 bodies. This inference is supported by the lack of V isotope fractionation observed during
347 hydrothermal alteration of terrestrial rocks (Prytulak et al., 2013). Furthermore, our data set for L
348 chondrites cover a wide range of metamorphic grades from L3.0 to L6 (Table 1), which reveals
349 no V isotope fractionation during parent body metamorphism. Lastly, we can also investigate
350 potential nebular or parent body condensation/evaporation processes by normalizing the V
351 concentrations in the carbonaceous chondrites to those of significantly more refractory element
352 such as Al (Fig. 1a). However, all carbonaceous chondrites investigated here exhibit Al/V ratios
353 within error of each other, suggesting that partial condensation or volatilization of V was not
354 significant on carbonaceous chondrite parent bodies and is not the principle cause of the
355 observed V isotope variation. Similarly there is no correlation with an indicator of volatile
356 element depletion such as Al/Mn ratios (Fig. 1b)

357 An alternative isotope fractionation mechanism could occur due to redox gradients in a
358 parent body, where V isotopes potentially would be redistributed across these boundaries. Such a
359 process might explain why CK chondrites preserve the lightest V isotope composition among

carbonaceous chondrites (Table 1), because CK chondrites represent the most oxidized carbonaceous chondrite parent body (Kallemeyn et al., 1991; Righter and Neff, 2007). However, the Rumuruti chondrites represent one of the most oxidized meteorite parent bodies (Kallemeyn et al., 1996) and the R3.9 NWA 753 does not exhibit V isotope compositions lighter than other chondrites (ordinary or carbonaceous), which would argue against redox-driven V isotope fractionation processes. This conclusion is furthermore supported because many redox-driven processes inferred to operate on parent bodies manifest themselves through fluid metasomatism/metamorphism (Wang and Lipschutz, 2007; Wombacher et al., 2008), which we argued above does not cause V isotope fractionation based on the invariable V isotope compositions observed in L chondrites as well as altered terrestrial basalts.

4.2. Variable proportions of irradiated material

Several theoretical studies have predicted that refractory inclusions should be enriched in ^{50}V relative to average chondrite material due to production during irradiation with high-energy particles during the T-Tauri phase of the sun (Gounelle et al., 2006; Lee et al., 1998). The production of ^{50}V has been a particular focus primarily because the extremely high natural $^{51}V/^{50}V$ ratio (~415), which registers a larger change in the ratio for a small amount of ^{50}V produced. The theoretical calculations appear to be supported by recently published V isotope data for a small set of CAIs that exhibit values that range from broadly chondritic to as light as $\delta^{51}V_{AA}$ = -5.7‰ (Sossi et al., 2017). Given that CAIs generally contain V abundances up to approximately ten times higher than chondrites (Sylvester et al., 1993), it might be inferred that heterogeneous distribution of CAIs and other refractory inclusions should generally lead to lighter V isotope compositions in carbonaceous chondrites that contain the largest proportions of

refractory inclusions. However, the lightest V isotope compositions recorded here are found in CK chondrites that are reported to contain the lowest abundances of refractory inclusions of all carbonaceous chondrites (Kallemeyn et al., 1991), which would suggest that V isotopes in the bulk chondrites studied here are not controlled by the abundance of refractory inclusions. Of course, distribution of refractory inclusions in carbonaceous chondrites is highly heterogeneous and it is possible that our V isotope data simply reflect higher proportions of refractory inclusions in the CK and CO fragments analyzed relative to CV, CM and CR fragments. However, if refractory inclusions would exert the primary control on the observed V isotope variations, then it seems fortuitous that multiple fragments of three different CO chondrites all display the exact same V isotope composition, since it would suggest that these all had a small, but identical amount of refractory inclusion included within them. In addition, we also measured two different fragments of five of the carbonaceous chondrites studied here (Table 1). These duplicate fragments all exhibit identical V isotope compositions, which, like the arguments presented for the CK and CO chondrites, would require the exact same amount of refractory inclusions in the two fragments of each meteorite. Given the generally heterogeneous distribution of refractory inclusions in carbonaceous chondrites we, therefore, consider that irradiated refractory inclusions enriched in ^{50}V are unlikely to be the cause of the observed V isotope variation in carbonaceous chondrites. Although Sossi et al. (2017) report CAIs with very light V isotope compositions, it is important to note that the lightest CAIs they report are fine grained that also contain the lowest V concentrations (~80-90μg/g). Other CAIs may contain up to 1000μg/g (Sylvester et al., 1993), but the data of Sossi et al. (2017) would suggest that such CAIs are not isotopically light. Since V concentrations in carbonaceous chondrites are similar to the fine-grained CAIs, it would require >6% contamination of isotopically light CAI material in

our bulk carbonaceous chondrite samples to cause ~0.2‰ offset from the carbonaceous matrix, which would be easily detectable in the concentrations of highly refractory elements such as REEs, Ca and Al. However, none of our carbonaceous chondrites exhibit anomalously high refractory element concentrations compared with average carbonaceous chondrites (Table S2).

Together, we consider that the arguments presented above render it highly unlikely that our bulk chondrite V isotope variations are due to variable amounts of CAI contamination. However, this conclusion does not negate the possibility that irradiation could have played a role in producing the V isotope variations observed in CAIs.

4.3. Heterogeneous distribution of nucleosynthetically anomalous phases

Bulk meteorites representing everything from chondrite parent bodies to differentiated planets retain mass independent isotopic variations that likely reflect heterogeneous distribution of presolar grains with highly anomalous compositions (e.g. Carlson et al., 2007; Rotaru et al., 1992). One of the isotopes for which these variations are best preserved is ^{54}Cr (reported as $\varepsilon^{54}Cr = 10000 \times (^{54}Cr/^{52}Cr_{sample} - ^{54}Cr/^{52}Cr_{std})/^{54}Cr/^{52}Cr_{std}$ where Earth by definition has the value 0) that exhibit both excesses and deficits in bulk meteorites relative to Earth (Qin et al., 2010; Sugiura and Fujiya, 2014; Trinquier et al., 2007). The V isotope compositions of the different carbonaceous chondrite classes show a positive correlation with $\varepsilon^{54}Cr$ anomalies (Fig. 2), which implies a common origin for the variation of the two isotope systems. Here, we use the average $\varepsilon^{54}Cr$ for chondrite groups when there are at least two separate measurements reported, except for the CK5 chondrite EET92002, where we use the actual value reported for this meteorite (Qin et al., 2010). The approach of using group averages is justified because each group displays no $\varepsilon^{54}Cr$ variation outside of reported analytical errors. It is, therefore, reasonable to assume that all

429 members of each group exhibit identical $\varepsilon^{54}Cr$. The consistent V isotope compositions of
430 different members of the same group further supports the idea of a relatively homogenous V
431 isotope composition for each group and the notion that $\varepsilon^{54}Cr$ and $\delta^{51}V_{AA}$ can be plotted against
432 each other for different chondrite groups.

433 The largest bulk meteorite excesses in ^{54}Cr are observed for the carbonaceous chondrites
434 (Qin et al., 2010; Sugiura and Fujiya, 2014; Trinquier et al., 2007) and since ^{54}Cr is the most
435 neutron-rich isotope of Cr these excesses are often interpreted to reflect addition of material
436 produced by the r-process (rapid neutron capture) in supernovae (e.g. Trinquier et al., 2007) or
437 through production in AGB stars (Wasserburg et al., 2015). This interpretation is consistent with
438 the finding of very large ^{54}Cr excesses in spinel presolar grains from carbonaceous chondrites
439 that likely originated from a supernova (Dauphas et al., 2010). The positive correlation we report
440 here between $\varepsilon^{54}Cr$ and $\delta^{51}V$ would furthermore support an r-process origin for these two isotope
441 ratios given that ^{51}V is also the most neutron-rich isotope of V and not shielded by another
442 isotope during neutron capture processes. Lastly, since Cr and V both have strong affinities for
443 chromian spinel (Canil, 1999; Righter et al., 2006) and aluminous spinal (Connolly and Burnett,
444 2003) it is reasonable to infer the same carrier phase for neutron-rich isotopes of these two
445 elements. Other host phases cannot be ruled out, however, since V concentrations in silicon
446 carbide (SiC), diamond and graphite (the most common presolar grains) is unknown. However,
447 to our knowledge no V isotope data exist for pre-solar grains. Hence, future work should focus
448 on testing the pre-solar grain origin of the V-Cr isotope correlation.

449 On the other hand, the negative correlation between the neutron rich isotopes ^{54}Cr and ^{50}Ti
450 in bulk carbonaceous chondrites (Trinquier et al., 2009; Warren, 2011) potentially contradicts the
451 r-process origin of the excess in ^{54}Cr and ^{51}V. But Ti is not compatible in chromian or aluminous

spinel (Canil, 2002), and so Ti may be somewhat decoupled from Cr and V isotopic correlations if chromian spinel is the primary host phase of V. The same argument is also likely to hold true for other isotope systems that display the dichotomy between carbonaceous and non-carbonaceous meteorites such as Ru and Mo (Budde et al., 2016; Fischer-Gödde and Kleine, 2017; Poole et al., 2017). Correlations do exist between ^{54}Cr and ^{50}Ti anomalies in bulk meteorites so chromian spinel is unlikely to be the sole host phase for Cr. However, given the substantial scatter in the correlations between bulk meteorite ^{54}Cr and ^{50}Ti anomalies, it is reasonable to infer that pre-solar Cr and Ti is not predominantly hosted by the same mineral phase.

If we, alternatively, assume that CI chondrites represent the solar value undiluted by supernova ejecta, then we can reproduce the positive correlation between ε^{54}Cr anomalies and ^{51}V/^{50}V by mixing solar material with calculated supernova ejecta (Figs. 2 and 3) because these predominantly are depleted in ^{54}Cr and ^{51}V relative to the average solar system (Rauscher et al., 2002; Woosley et al., 2002). These mixing calculations take into account the isotopic make-up as well as abundances in different models of supernova ejecta (Rauscher et al., 2002; Woosley et al., 2002) and the bulk solar system (Lodders, 2003). However, calculations of isotope compositions in supernova ejecta generally do not include specific calculations of the r-process (Rauscher et al., 2002; Woosley et al., 2002), which complicates application of the mixing relationships presented in Figures 2 and 3. On the other hand, isotopes with masses below 56 atomic mass units can be produced by multiple other processes than neutron capture (Rauscher et al., 2002; Woosley et al., 2002), which suggests that such isotopes in supernova ejecta might not necessarily be dominated by r-process neutron capture and hence calculations that do not include the r-process material could still account for some of the characteristics observed in bulk

carbonaceous chondrites. Irrespective of the ultimate origin of the correlated $\varepsilon^{54}Cr$ and $\delta^{51}V$ ratios, considerations of r-process neutron capture and calculated supernova ejecta both support a nucleosynthetic origin for the V isotope variations.

5. The non-carbonaceous or non-chondritic Earth?

The difference between BSE and chondritic meteorites could have been produced by stable V isotope fractionation during terrestrial core formation. Given the V mass balance of Earth (Wade and Wood, 2005), the heavier V isotope composition found here for chondrites would require a fractionation factor between core and mantle of 0.6‰ to 0.8‰, which is significantly smaller than the 1.4‰ to 1.9‰ required by previous meteorite data (Nielsen et al., 2014). However, simple metal-silicate equilibration experiments reveal no detectable V isotope fractionation within the uncertainty of ~0.2‰ (Nielsen et al., 2014), which is consistent with for example the magnitude of isotope fractionation predicted for Fe during partitioning into the core (Polyakov, 2009). Therefore, terrestrial core formation is unlikely to account for the BSE-chondrite difference in V isotopes.

There is ongoing debate regarding the origin of the material that forms the primary building blocks of Earth (Budde et al., 2016; Burkhardt et al., 2016; Burkhardt et al., 2011; Fitoussi and Bourdon, 2012; Warren, 2011). Both mass dependent and independent isotope tracers have been employed to investigate whether Earth could have been constructed from mixtures of chondritic meteorites or potentially must also encompass material not found in our meteorite collections. For example, bulk meteorite anomalies of nucleosynthetic Nd and Mo isotopes reveal that Earth plots at the end of the spectra of values recorded (Burkhardt et al., 2016; Burkhardt et al., 2011; Poole et al., 2017), which suggests that Earth cannot be made exclusively from realistic mixtures

498 of known chondritic meteorite reservoirs. Similarly, the vanadium isotope composition of silicate
499 Earth estimated from a small set of whole rock peridotite data ($\delta^{51}V_{AA}$ = -0.7 ± 0.2‰; (Prytulak
500 et al., 2013)) is still heavier than all the meteorite classes investigated here, which also requires a
501 non-chondritic origin for much of Earth's building blocks.

502 At the same time, large data sets for bulk meteorite isotope anomalies of ^{54}Cr, ^{50}Ti, and ^{17}O
503 clearly shows a dichotomy between carbonaceous chondrites that plot on one trend and most
504 differentiated planetesimals and ordinary chondrites that plot on a different correlation line
505 (Warren, 2011). These isotopic groupings could be linked to the presence of a physical barrier in
506 the early solar system that prevented the carbonaceous and non-carbonaceous bodies from being
507 mixed (Kruijer et al., 2017) until giant planet migration or some other process brought the two
508 reservoirs back into contact around 3-4 million years after the start of the solar system (Sarafian
509 et al., 2017). In addition to the carbonaceous chondrites, our data for L, H, and E chondrites can
510 together with Earth be matched with corresponding ε^{54}Cr data because these meteorite groups
511 display very little ε^{54}Cr variation (Qin et al., 2010; Sugiura and Fujiya, 2014) and we can
512 therefore assume that the samples investigated here for V isotopes record ε^{54}Cr-values similar to
513 other L, H, and E chondrites. We do not attempt to plot R chondrites because only a single R
514 chondrite has been measured for ε^{54}Cr and it is unknown if different R chondrites preserve large
515 ε^{54}Cr variations. Although less pronounced than for carbonaceous chondrites, a shallow
516 correlation between Earth, L, H, and E chondrites might be present (Fig. 2). Undoubtedly,
517 additional coupled V and Cr isotope measurements for non-carbonaceous meteorites are required
518 to assess how robust the correlation is, but in its current form the trend suggests that although V
519 isotopes overlap between the carbonaceous and non-carbonaceous meteorites, Earth falls on the
520 extension of the non-carbonaceous trend at a V isotope composition that is heavier than any

meteorite analyzed to date. As such, V isotopes support that Earth formed primarily from a reservoir that did not contain carbonaceous chondrites, while, similarly to nucleosynthetic Nd and Mo isotopes, implying that there appears to be a portion of the non-carbonaceous reservoir that Earth is the only known representative of.

6. Acknowledgements

This study was funded by NASA Emerging Worlds grant NNX16AD36G to SGN. We thank the Harvard Natural History Museum, NASA-JSC and Tom Lapen for access to meteorite samples. US Antarctic meteorite samples are recovered by the Antarctic Search for Meteorites (ANSMET) program, which has been funded by NSF and NASA, and characterized and curated by the Astromaterials Curation Office at NASA Johnson Space Center and the Department of Mineral Sciences of the Smithsonian Institution. J. Blusztajn is thanked for help with mass spectrometry support at WHOI. S. Page and D. Novella are thanked for help in processing and measuring intercalibration samples alongside B.J. Coles for mass spectrometry support at Imperial College London with support from NERC grant NE/N009568/1 to JP.

7. References

Budde, G., Burkhardt, C., Brennecka, G.A., Fischer-Godde, M., Kruijer, T.S., Kleine, T., 2016. Molybdenum isotopic evidence for the origin of chondrules and a distinct genetic heritage of carbonaceous and non-carbonaceous meteorites. Earth Planet. Sci. Lett. 454, 293-303.

Burkhardt, C., Borg, L.E., Brennecka, G.A., Shollenberger, Q.R., Dauphas, N., Kleine, T., 2016. A nucleosynthetic origin for the Earth's anomalous Nd-142 composition. Nature 537, 394-398.

Burkhardt, C., Kleine, T., Oberli, F., Pack, A., Bourdon, B., Wieler, R., 2011. Molybdenum isotope anomalies in meteorites: Constraints on solar nebula evolution and origin of the Earth. Earth Planet. Sci. Lett. 312, 390-400.

Burnett, D.S., Fowler, W.A., Hoyle, F., 1965. Nucleosynthesis in the early history of the solar system. Geochim. Cosmochim. Acta. 29, 1209-1241.

548 Canil, D., 1999. Vanadium partitioning between orthopyroxene, spinel and silicate melt and the
549 redox states of mantle source regions for primary magmas. Geochim. Cosmochim. Acta. 63, 557-
550 572.
551 Canil, D., 2002. Vanadium in peridotites, mantle redox and tectonic environments: Archean to
552 present. Earth Planet. Sci. Lett. 195, 75-90.
553 Carlson, R.W., Boyet, M., Horan, M., 2007. Chondrite barium, neodymium, and samarium
554 isotopic heterogeneity and early earth differentiation. Science 316, 1175-1178.
555 Chaussidon, M., Robert, F., McKeegan, K.D., 2006. Li and B isotopic variations in an Allende
556 CAI: Evidence for the in situ decay of short-lived Be-10 and for the possible presence of the
557 short-lived nuclide Be-7 in the early solar system. Geochim. Cosmochim. Acta. 70, 224-245.
558 Clayton, R.N., 1993. Oxygen Isotopes in Meteorites. Annu. Rev. Earth Planet. Sci. 21, 115-149.
559 Connolly, H.C., Burnett, D.S., 2003. On type B CAI formation: experimental constraints on fO2
560 variations in spinel minor element partitioning and reequilibration effects. Geochim.
561 Cosmochim. Acta. 67, 4429-4434.
562 Dauphas, N., Remusat, L., Chen, J.H., Roskosz, M., Papanastassiou, D.A., Stodolna, J., Guan,
563 Y., Ma, C., Eiler, J.M., 2010. Neutron-rich Chromium Isotope Anomalies in Supernova
564 Nanoparticles. The Astrophysical Journal 720, 1577.
565 Desch, S.J., Morris, M.A., Connolly, H.C., Jr., Boss, A.P., 2010. A critical examination of the X-
566 wind model for chondrule and calcium-rich, aluminum-rich inclusion formation and radionuclide
567 production. Astrophys. J. 725, 692-711.
568 Feigelson, E.D., 2010. X-ray insights into star and planet formation. P Natl Acad Sci USA 107,
569 7153-7157.
570 Fischer-Gödde, M., Kleine, T., 2017. Ruthenium isotopic evidence for an inner Solar System
571 origin of the late veneer. Nature 541, 525.
572 Fitoussi, C., Bourdon, B., 2012. Silicon Isotope Evidence Against an Enstatite Chondrite Earth.
573 Science 335, 1477-1480.
574 Gerber, S., Burkhardt, C., Budde, G., Metzler, K., Kleine, T., 2017. Mixing and Transport of
575 Dust in the Early Solar Nebula as Inferred from Titanium Isotope Variations among Chondrules.
576 Astrophys. J. Lett. 841.
577 Gounelle, M., Shu, F.H., Shang, H., Glassgold, A.E., Rehm, K.E., Lee, T., 2006. The irradiation
578 origin of beryllium radioisotopes and other short-lived radionuclides. Astrophys. J. 640, 1163-
579 1170.
580 Hopkins, S.S., Prytulak, J., Barling, J., Russell, S.S., Coles, B.J., Halliday, A.N., 2018. The
581 vanadium isotopic composition of lunar basalts. Earth Planet. Sci. Lett. submitted.
582 Kallemeyn, G.W., Rubin, A.E., Wasson, J.T., 1991. The Compositional Classification of
583 Chondrites .5. The Karoonda (Ck) Group of Carbonaceous Chondrites. Geochim. Cosmochim.
584 Acta. 55, 881-892.
585 Kallemeyn, G.W., Rubin, A.E., Wasson, J.T., 1996. The compositional classification of
586 chondrites .7. The R chondrite group. Geochim. Cosmochim. Acta. 60, 2243-2256.
587 Kelley, K.A., Plank, T., Ludden, J., Staudigel, H., 2003. Composition of altered oceanic crust at
588 ODP Sites 801 and 1149. Geochem. Geophys. Geosyst. 4.
589 Kruijer, T.S., Burkhardt, C., Budde, G., Kleine, T., 2017. Age of Jupiter inferred from the
590 distinct genetics and formation times of meteorites. P Natl Acad Sci USA 114, 6712-6716.
591 Lee, T., Shu, F.H., Shang, H., Glassgold, A.E., Rehm, K.E., 1998. Protostellar cosmic rays and
592 extinct radioactivities in meteorites. Astrophys. J. 506, 898-912.

Lodders, K., 2003. Solar system abundances and condensation temperatures of the elements. Astrophys. J. 591, 1220-1247.
McKeegan, K.D., Chaussidon, M., Robert, F., 2000. Incorporation of short-lived Be-10 in a calcium-aluminum-rich inclusion from the Allende meteorite. Science 289, 1334-1337.
Morbidelli, A., Chambers, J., Lunine, J.I., Petit, J.M., Robert, F., Valsecchi, G.B., Cyr, K.E., 2000. Source regions and timescales for the delivery of water to the Earth. Meteorit. Planet. Sci. 35, 1309-1320.
Morbidelli, A., Lunine, J.I., O'Brien, D.P., Raymond, S.N., Walsh, K.J., 2012. Building Terrestrial Planets. Annu Rev Earth Pl Sc 40, 251-275.
Moynier, F., Paniello, R.C., Gounelle, M., Albarede, F., Beck, P., Podosek, F., Zanda, B., 2011. Nature of volatile depletion and genetic relationships in enstatite chondrites and aubrites inferred from Zn isotopes. Geochim. Cosmochim. Acta. 75, 297-307.
Nielsen, S.G., Owens, J.D., Horner, T.J., 2016. Analysis of high-precision vanadium isotope ratios by medium resolution MC-ICP-MS. J. Anal. At. Spectrom. 31, 531-536.
Nielsen, S.G., Prytulak, J., Halliday, A.N., 2011. Determination of Precise and Accurate 51V / 50V Isotope Ratios by MC-ICP-MS, Part 1: Chemical Separation of Vanadium and Mass Spectrometric Protocols. Geostand. Geoanal. Res. 35, 293-306.
Nielsen, S.G., Prytulak, J., Wood, B.J., Halliday, A.N., 2014. Vanadium isotopic difference between the silicate Earth and meteorites. Earth Planet. Sci. Lett. 389, 167-175.
Polyakov, V.B., 2009. Equilibrium Iron Isotope Fractionation at Core-Mantle Boundary Conditions. Science 323, 912-914.
Poole, G.M., Rehkamper, M., Coles, B.J., Goldberg, T., Smith, C.L., 2017. Nucleosynthetic molybdenum isotope anomalies in iron meteorites - new evidence for thermal processing of solar nebula material. Earth Planet. Sci. Lett. 473, 215-226.
Prytulak, J., Nielsen, S.G., Halliday, A.N., 2011. Determination of Precise and Accurate 51V / 50V Isotope Ratios by Multi-Collector ICP-MS, Part 2: Isotopic Composition of Six Reference Materials plus the Allende Chondrite and Verification Tests. Geostand. Geoanal. Res. 35, 307-318.
Prytulak, J., Nielsen, S.G., Ionov, D.A., Halliday, A.N., Harvey, J., Kelley, K.A., Niu, Y., Peate, D.W., Shimizu, K., Sims, K.W.W., 2013. The Stable Vanadium Isotope Composition of the Mantle and Mafic Lavas. Earth Planet. Sci. Lett. 365, 177-189.
Prytulak, J., Sossi, P.A., Halliday, A.N., Plank, T., Savage, P.S., Woodhead, J.D., 2017. Stable vanadium isotopes as a redox proxy in magmatic systems? Geochemical Perspectives Letters 3, 75-84.
Qin, L.P., Alexander, C.M.O., Carlson, R.W., Horan, M.F., Yokoyama, T., 2010. Contributors to chromium isotope variation of meteorites. Geochim. Cosmochim. Acta. 74, 1122-1145.
Rauscher, T., Heger, A., Hoffman, R.D., Woosley, S.E., 2002. Nucleosynthesis in massive stars with improved nuclear and stellar physics. Astrophys. J. 576, 323-348.
Righter, K., Leeman, W.P., Hervig, R.L., 2006. Partitioning of Ni, Co and V between spinel-structured oxides and silicate melts: Importance of spinel composition. Chem. Geol. 227, 1-25.
Righter, K., Neff, K.E., 2007. Temperature and oxygen fugacity constraints on CK and R chondrites and implications for water and oxidation in the early solar system. Polar Science 1, 25-44.
Robert, F., Gautier, D., Dubrulle, B., 2000. The solar system D/H ratio: Observations and theories. Space Sci Rev 92, 201-224.

638 Rotaru, M., Birck, J.L., Allegre, C.J., 1992. Clues to Early Solar-System History from
639 Chromium Isotopes in Carbonaceous Chondrites. Nature 358, 465-470.
640 Sarafian, A.R., Nielsen, S.G., Marschall, H.R., Gaetani, G.A., Hauri, E.H., Righter, K., Sarafian,
641 E., 2017. Angrite meteorites record the onset and flux of water to the inner solar system.
642 Geochim. Cosmochim. Acta. 212, 156-166.
643 Schuth, S., Horn, I., Bruske, A., Wolff, P.E., Weyer, S., 2017. First vanadium isotope analyses of
644 V-rich minerals by femtosecond laser ablation and solution-nebulization MC-ICP-MS. Ore Geol
645 Rev 81, 1271-1286.
646 Sears, D.W.G., Weeks, K.S., 1983. Chemical and Physical Studies of Type-3 Chondrites .2.
647 Thermo-Luminescence of 16 Type-3 Ordinary Chondrites and Relationships with Oxygen
648 Isotopes. Journal of Geophysical Research 88, B301-B311.
649 Sears, D.W.G., Weeks, K.S., 1986. Chemical and Physical Studies of Type-3 Chondrites .6.
650 Siderophile Elements in Ordinary Chondrites. Geochim. Cosmochim. Acta. 50, 2815-2832.
651 Shen, J.J.S., Lee, T., Chang, C.T., 1994. Lanthanum Isotopic Composition of Meteoritic and
652 Terrestrial Matter. Geochim. Cosmochim. Acta. 58, 1499-1506.
653 Shu, F.H., Shang, H., Glassgold, A.E., Lee, T., 1997. X-rays and fluctuating x-winds from
654 protostars. Science 277, 1475-1479.
655 Shu, F.H., Shang, H., Gounelle, M., Glassgold, A.E., Lee, T., 2001. The origin of chondrules and
656 refractory inclusions in chondritic meteorites. Astrophys. J. 548, 1029-1050.
657 Shukolyukov, A., Lugmair, G.W., 2006. Manganese-chromium isotope systematics of
658 carbonaceous chondrites. Earth Planet. Sci. Lett. 250, 200-213.
659 Sossi, P.A., Moynier, F., Chaussidon, M., Villeneuve, J., Kato, C., Gounelle, M., 2017. Early
660 Solar System irradiation quantified by linked vanadium and beryllium isotope variations in
661 meteorites. Nature Astronomy 1, 0055.
662 Sossi, P.A., Prytulak, J., O'Neill, H.S.C., 2018. Experimental calibration of vanadium
663 partitioning and stable isotope fractionation between hydrous granitic melt and magnetite at
664 800C and 0.5 GPa. Contrib. Mineral. Petrol. 173.
665 Sugiura, N., Fujiya, W., 2014. Correlated accretion ages and epsilon Cr-54 of meteorite parent
666 bodies and the evolution of the solar nebula. Meteorit. Planet. Sci. 49, 772-787.
667 Sylvester, P.J., Simon, S.B., Grossman, L., 1993. Refractory inclusions from the Leoville,
668 Efremovka, and Vigarano c3v chondrites: Major element differences between types A and B,
669 and extraordinary refractory siderophile element compositions. Geochim. Cosmochim. Acta. 57,
670 3763-3784.
671 Trinquier, A., Birck, J.L., Allegre, C.J., 2007. Widespread Cr-54 heterogeneity in the inner solar
672 system. Astrophys. J. 655, 1179-1185.
673 Trinquier, A., Elliott, T., Ulfbeck, D., Coath, C., Krot, A.N., Bizzarro, M., 2009. Origin of
674 Nucleosynthetic Isotope Heterogeneity in the Solar Protoplanetary Disk. Science 324, 374-376.
675 Wade, J., Wood, B.J., 2005. Core formation and the oxidation state of the Earth. Earth Planet.
676 Sci. Lett. 236, 78-95.
677 Wang, M.S., Lipschutz, M.E., 2007. Trace elements in primitive meteorites - VII Antarctic
678 unequilibrated ordinary chondrites. Geochim. Cosmochim. Acta. 71, 1062-1073.
679 Warren, P.H., 2011. Stable-isotopic anomalies and the accretionary assemblage of the Earth and
680 Mars: A subordinate role for carbonaceous chondrites. Earth Planet. Sci. Lett. 311, 93-100.
681 Wasserburg, G.J., Trippella, O., Busso, M., 2015. Isotope Anomalies in the Fe-group Elements
682 in Meteorites and Connections to Nucleosynthesis in AGB Stars. The Astrophysical Journal 805,
683 7.

Wombacher, F., Rehkämper, M., Mezger, K., Bischoff, A., Münker, C., 2008. Cadmium stable isotope cosmochemistry. Geochim. Cosmochim. Acta. 72, 646-667.
Wood, J.A., 2004. Formation of chondritic refractory inclusions: the astrophysical settings. Geochim. Cosmochim. Acta. 68, 4007-4021.
Woodhead, J., Hergt, J., 2000. Pb-isotope analyses of USGS reference materials. Geostand. Geoanal. Res. 24, 33-38.
Woosley, S.E., Heger, A., Weaver, T.A., 2002. The evolution and explosion of massive stars. Rev Mod Phys 74, 1015-1071.
Wu, F., Owens, J.D., Huang, T., Sarafian, A.R., Huang, K.F., Sen, I., Horner, T.J., Blusztajn, J., Morton, P.M., Nielsen, S.G., 2018a. Vanadium Isotope Composition of Seawater. Geochim. Cosmochim. Acta. in press.
Wu, F., Qi, Y., Perfit, M.R., Gao, Y., Langmuir, C.H., Wanless, V.D., Yu, H., Huang, F., 2018b. Vanadium isotope compositions of mid-ocean ridge lavas and altered oceanic crust. Earth Planet. Sci. Lett. 493, 128-139.
Wu, F., Qi, Y.H., Yu, H.M., Tian, S.Y., Hou, Z.H., Huang, F., 2016. Vanadium isotope measurement by MC-ICP-MS. Chem. Geol. 421, 17-25.
Wu, F., Qin, T., Li, X.F., Liu, Y., Huang, J.H., Wu, Z.Q., Huang, F., 2015. First-principles investigation of vanadium isotope fractionation in solution and during adsorption. Earth Planet. Sci. Lett. 426, 216-224.
York, D., Evensen, N.M., Martinez, M.L., Delgado, J.D., 2004. Unified equations for the slope, intercept, and standard errors of the best straight line. Am J Phys 72, 367-375.
Zinner, E., 1998. Stellar nucleosynthesis and the isotopic composition of presolar grains from primitive meteorites. Annu. Rev. Earth Planet. Sci. 26, 147-188.

Table 1: Vanadium isotope data for chondrites

Sample	Type	source	V (μg/g)	$\delta^{51}V_{AA}$	2SD	2SE	analyses	splits	chips
Carbonaceous chondrites									
ALH83100	CM1/2	MWG	73	-1.07	0.18		7	2	1
Mighei	CM2	HMNH	*59*	-1.05	0.10		2	1	1
CM average				**-1.07**		**0.06**	**9**		
LAP 02206	CV3	MWG	88	-1.09	0.10		7	2	2
LAR 12002	CV3	MWG	90	-1.20	0.10		4	1	1
CV average				**-1.13**		**0.04**	**11**		
DOM 08006	CO3	MWG	81	-1.22	0.10		10	4	2
Lance	CO3.5	HMNH	75	-1.22	0.26		19	7	1
Warrenton	CO3.7	HMNH	*76*	-1.24	0.11		9	3	1
CO average				**-1.22**		**0.03**	**37**		
MIL 09001	CR2	MWG	68	-1.22	0.15		10	3	2
GRA 06100	CR2	MWG	70	-1.07	0.23		9	2	2
CR average				**-1.15**		**0.06**	**19**		
EET 92002	CK5	MWG	92	-1.32	0.15		9	3	2
CK average				**-1.32**		**0.05**	**9**		
Ordinary chondrites									
QUE 97008	L3.0	MWG	69	-1.22	0.21		5	2	1
GRO 06054	L3.6	MWG	82	-1.33	0.10		6	2	1
GRO 95515	L4	MWG	*71*	-1.20	0.10		3	1	1
Borkut	L5	HMNH	*95*	-1.12	0.10		2	1	1
Alfianello	L6	HMNH	66	-1.24	0.10		7	2	1
Calliham	L6	HMNH	63	-1.32	0.10		2	1	1
L average				**-1.25**		**0.03**	**25**		
WSG 95300	H3.3	MWG	66	-1.39	0.10		3	1	1
ALHA77215*	H3.7	MWG	69	-1.35	0.13		5	2	1
H average				**-1.37**		**0.04**	**8**		
MET 00452	LL/L3.05	MWG	70	-1.09	0.11		6	2	1
NWA 753	R3.9	purchase	77	-1.13	0.15		8	3	1
St Marks	EH5	T. Lapen	50	-1.05	0.10		4	1	1

MWG - Meteorite Working Group, NASA; HMNH - Harvard Museum of Natural History; NMNH - National Museum of Natural History

Concentrations in italics are based on column chemistry yield all others from ICP-MS (see supplement)

Analyses refer to the number of individual mass spectrometric analyses performed; ***splits*** refer to number of separate dissolved splits of meteorite processed through the entire ion exchange column procedure; ***chips*** refer to the number of different meteorite fragments dissolved separately and processed through the entire ion exchange column procedure

* - Sample originally classified as L3.8 chondrite, but previous studies (Sears and Weeks, 1983, 1986) as well as its elemental composition determined here (Table S2) imply it is an H chondrite.

Table 2: Interlaboratory comparison

Sample	Type	WHOI			FSU			ICL		
		$\delta^{51}V_{AA}$	2SD	n	$\delta^{51}V_{AA}$	2SD	n	$\delta^{51}V_{AA}$	2SD	n
DOM 08006	CO3	-1.25	0.10	5	-1.19	0.07	3	-1.21	0.15	2
NWA 753	R3.9	-1.14	0.15	4	-1.16	0.10	3	-0.97	0.15	1
BDH	V solution	-1.18	0.11	31	-1.18	0.10	6	-1.11	0.20	4

Uncertainties are calculated from the number of analyses conducted (n) except for the ICL meteorite analyses that apply the long-term external reproducibility of reference materials in that lab because only 1 or 2 analyses were performed.

731 Table 3: Vanadium isotope compositions of terrestrial silicate reference materials

Reference Material	$\delta^{51}V_{AA}$	2SD	Analyses	Splits	Reference
AGV-2					
	-0.73	0.17	16	7	WHOI (this study)
	-0.70	0.10	37	n.g.	Wu et al. (2016)
	-0.50	0.19	4	4	Prytulak et al. (2011)
BCR-2					
	-0.79	0.15	24	10	WHOI (this study)
	-0.80	0.14	3	3	ICL (this study)
	-0.85	0.26	5	2	Hopkins et al. (submitted)
	-1.11	0.08	2	1	Sossi et al. (2018)
	-1.03	0.09	9	n.g.	Schuth et al. (2017)
	-0.78	0.08	36	n.g.	Wu et al. (2016)
	-0.95	0.16	27	12	Prytulak et al. (2011)
BHVO-2					
	-0.86	0.12	2	2	Hopkins et al. (submitted)
	-0.83	0.09	22	n.g.	Wu et al. (2016)
	-0.89	0.08	9	3	Prytulak et al (2011)
BIR1a					
	-0.89	0.23	3	2	Hopkins et al. (submitted)
	-1.05	0.22	7	3	Sossi et al. (2018)
	-0.92	0.09	52	n.g.	Wu et al. (2016)
	-0.94	0.15	52	10	Prytulak et al. (2011)
JA-2					
	-0.88	0.10	4	1	WHOI (this study)
	-0.80	0.07	13	n.g.	Wu et al. (2016)
GSP-2					
	-0.76	0.15	4	1	WHOI (this study)
	-0.62	0.07	26	n.g.	Wu et al. (2016)
	-0.63	0.10	6	3	Prytulak et al. (2011)

732 n.g. - information not provided

733 ***Analyses*** refer to the number of individual mass spectrometric analyses performed; ***splits*** refer to
734 number of separate dissolved splits of sample processed through the entire ion exchange column
735 procedure

736

Figure Captions:

Figure 1: *Vanadium isotope compositions of five carbonaceous chondrite groups investigated (CO, CM, CV, CK, and CR) plotted against their measured (a) Al/V and (b) Al/Mn ratios. The trace element concentrations were measured on splits of the same solutions that were processed for V isotopes. It is evident that there is no noticeable depletion in V relative to more refractory Al. Kinetic isotope fractionation during partial condensation/evaporation processes are, therefore, not likely to explain the observed V isotope variation. Concentrations of Al and other elements in the samples can be found in the supplement.*

Figure 2: *Vanadium isotopes plotted against $\varepsilon^{54}Cr$ isotope anomalies for the CO, CM, CV, CK, and CR carbonaceous chondrite groups. The Cr isotope data was taken from the literature (Qin et al., 2010; Shukolyukov and Lugmair, 2006; Trinquier et al., 2007) and represents group averages, except for CK chondrites where the $\varepsilon^{54}Cr$ value for EET 92002 was used (Qin et al., 2010). Also shown are mixing lines in V vs Cr isotopes between modeled supernova ejecta (Rauscher et al., 2002) and average solar material (Lodders, 2003). The $\delta^{51}V_{AA}$ value for CI chondrites was inferred based on the correlation between Cr and V isotopes and the known $\varepsilon^{54}Cr$ for CI chondrites (Shukolyukov and Lugmair, 2006; Trinquier et al., 2007). The mixing lines (red dashed, green bold and black dotted) are the same as shown in figure 3. Note that the slope of these mixing lines are somewhat different in the two figures because $\varepsilon^{54}Cr$ has been normalized to a solar $^{52}Cr/^{50}Cr$ ratio. Also shown are data points for E, L, H chondrites and Earth. Chromium isotope data for E, L and H chondrites are group averages based on literature data (Qin et al., 2010; Shukolyukov and Lugmair, 2006; Trinquier et al., 2007).*

Figure 3: *Comparison of $^{51}V/^{50}V$ and $^{54}Cr/^{52}Cr$ isotope ratios for models (small squares) of ejecta from supernova of massive stars between 15-25 solar masses (Rauscher et al., 2002) and the average solar composition (Lodders, 2003). Also shown are mixing lines (red dashed, green bold and black dotted) between three different supernova models (S15, S21 and S25 from Rauscher et al (2002)) and the solar composition.*

Figure 1
Click here to download Figure: Fig1_new.pdf

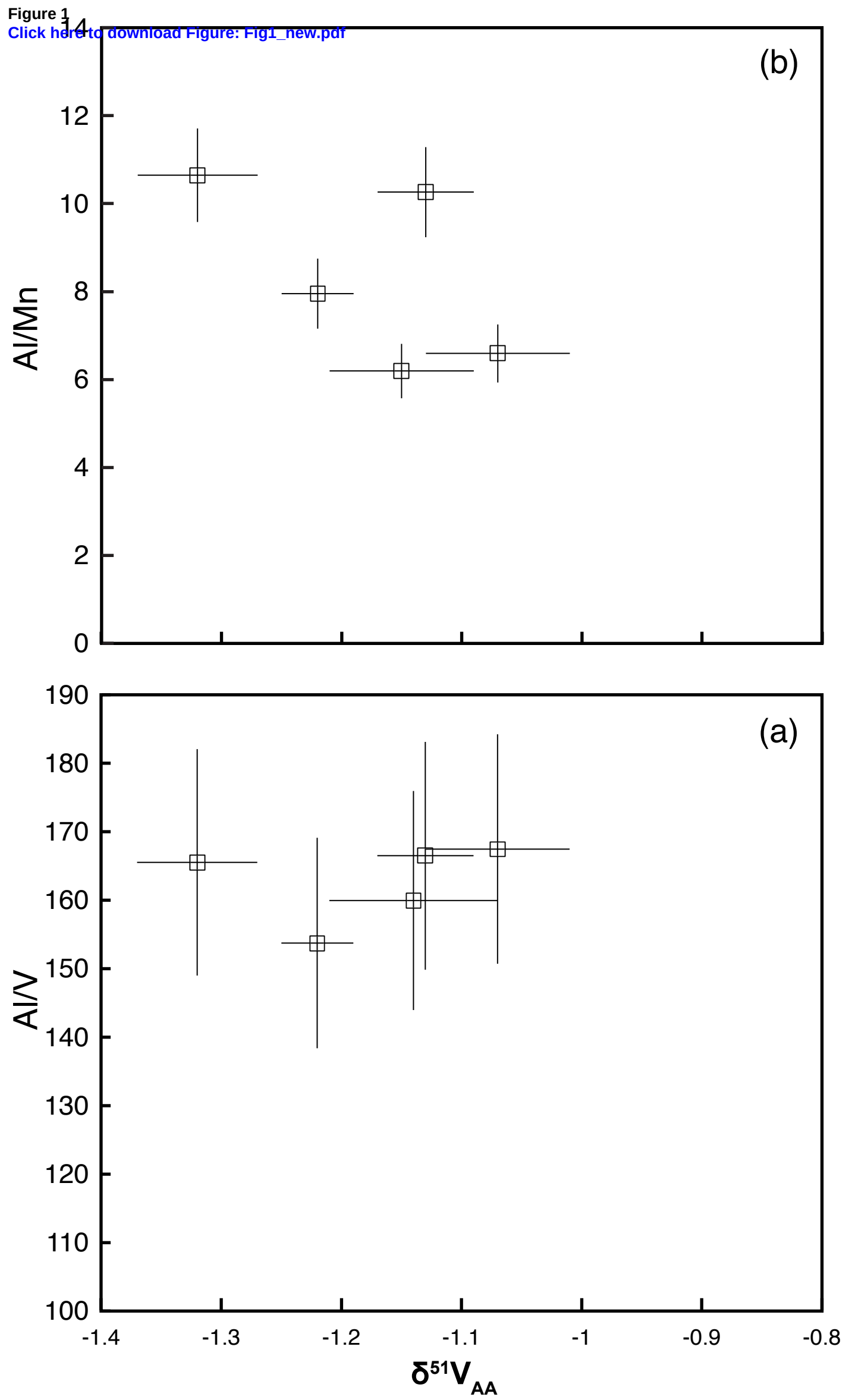

Figure 2
Click here to download Figure: Fig2.pdf

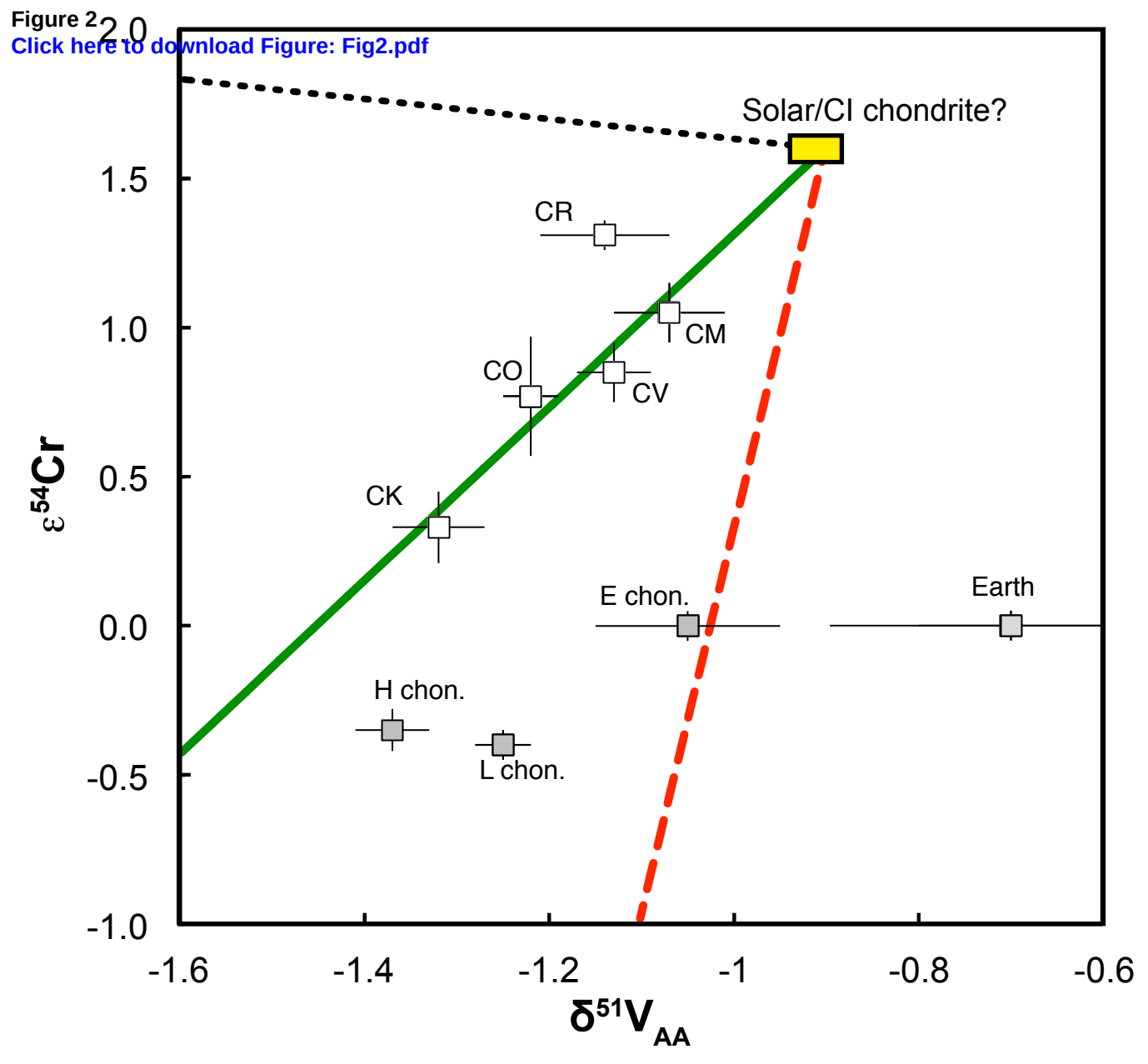

Figure 3

Click here to download Figure: Fig3.pdf

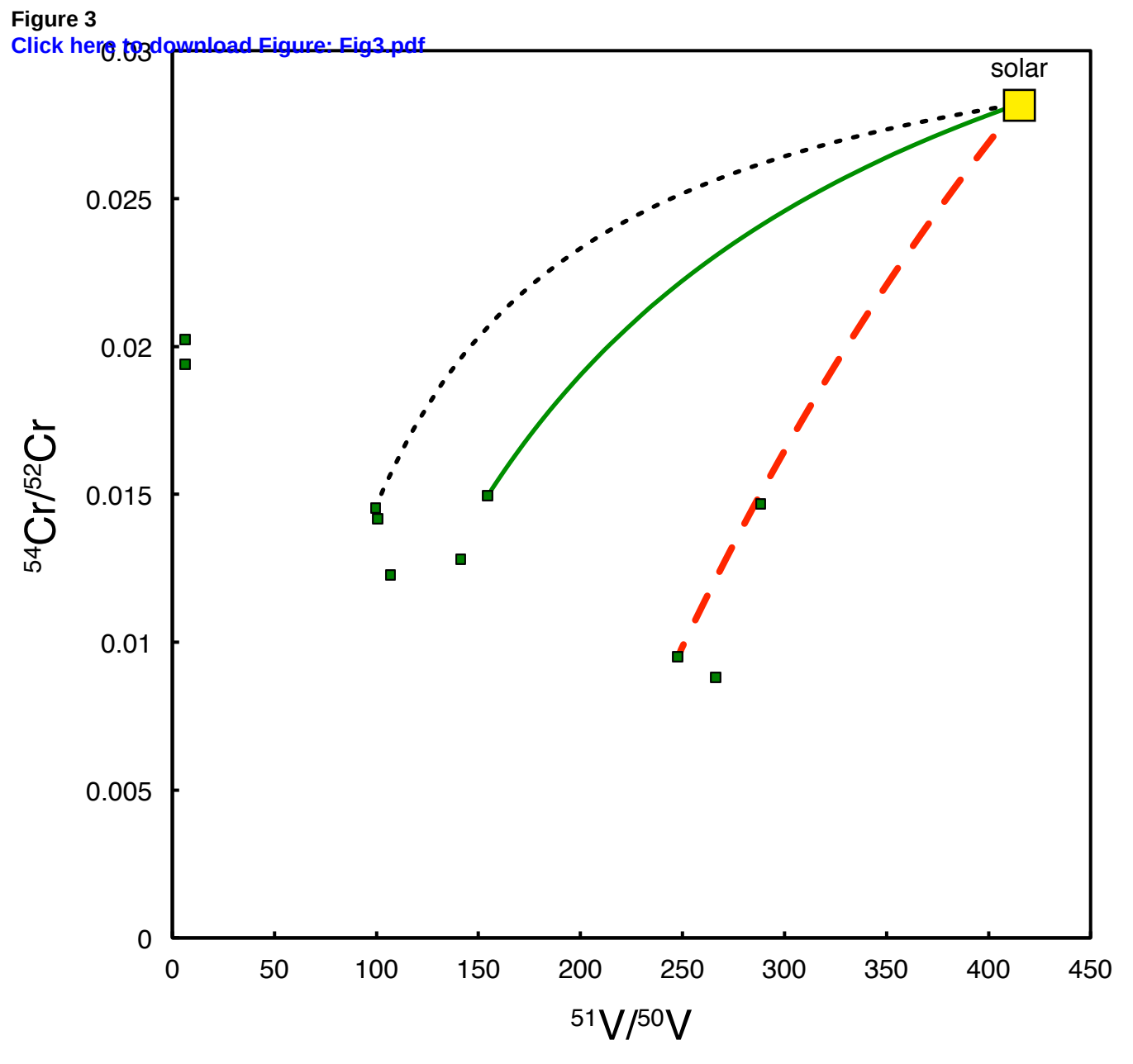

Supplementary material for online publication only

Click here to download Supplementary material for online publication only: Nielsen et al Supplement_revised.docx